Appl. Phys. B 73, 411–416 (2001)
DOI: 10.1007/s003400100719

Applied Physics B
Lasers and Optics

M. VOGEL[1]
K. HANSEN[2]
A. HERLERT[1]
L. SCHWEIKHARD[1,3,✉]

Energy dependence of the decay pathways of optically excited small gold clusters

[1] Institut für Physik, Johannes-Gutenberg-Universität Mainz, 55 099 Mainz, Germany
[2] Department of Physics, University of Jyväskylä, FIN-40 351 Jyväskylä, Finland
[3] Institut für Physik, Ernst-Moritz-Arndt-Universität, 17 487 Greifswald, Germany

Received: 9 July 2001/Revised version: 24 September 2001
Published online: 15 October 2001 •

ABSTRACT The pathway competition between neutral monomer and neutral dimer evaporation from optically excited odd-size gold cluster ions Au_n^+, $n = 7$–15, has been investigated as a function of cluster size and excitation energy. Gold cluster ions of these sizes are the only ones to show observable pathway competition while all other sizes exclusively evaporate either neutral monomers or neutral dimers. The investigation has been performed by photoexcitation of stored size-selected gold cluster ions with a single 10-ns laser pulse. Subsequent time-resolved observation of the delayed dissociation allows us to quantitatively determine the relative fragment yields of the respective decay channels as a function of excitation energy. Contrary to theoretical expectations, the dimer-to-monomer branching ratio of evaporated particles is found to decrease monotonously with increasing excitation energy for all cluster sizes under investigation. Possible explanations for this behaviour are discussed.

PACS 36.40.Qv; 36.40.Wa

1 Introduction

Numerous studies on the fragmentation pathways of singly charged metal clusters have been performed for several monovalent elements [1–12] and have proven to be an important tool in understanding cluster energetics and dynamics. After moderate excitation above their dissociation threshold the two possible decay pathways of singly charged monovalent metal cluster ions M_n^+ are the evaporation of a neutral monomer and the evaporation of a neutral dimer:

$$M_n^+ \nearrow M_{n-1}^+ + M \quad \searrow M_{n-2}^+ + M_2 \quad . \tag{1}$$

Significant odd–even alternations of the decay pathway branching ratio have been found for the clusters of the elements of group 1 and 11 (or 1B) of the periodic table and are a result of the clusters' electronic structure. Studies of the alkali-metal clusters Li_n^+ ($n = 4$–42) [1], Na_n^+ ($n = 5$–40) [2] and K_n^+ ($n = 5$–200) [3], and of the monovalent noble metal clusters Cu_n^+ ($n = 2$–17) [5, 12], Ag_n^+ ($n = 3$–21) [4, 6] and Au_n^+ ($n = 3$–23) [7] show that small odd-numbered clusters of these elements evaporate a neutral dimer while the other cluster sizes evaporate a neutral monomer. In all the cases mentioned, there is an intermediate size range of odd-numbered clusters where both decay pathways are observed to compete. A similar behavior has been found for anionic clusters, Cu_n^- ($n = 2$–8) [10], Ag_n^- ($n = 2$–11) [9] and Au_n^- ($n = 2$–15) [8, 11].

Recently, we have started a quantitative investigation of the branching ratio between monomer and dimer evaporation of positively charged gold clusters, Au_n^+ ($n = 2$–27) [13]. It is investigated by photofragmentation, specifically by time-resolved measurements of the delayed dissociation for $n = 7$–27. Small gold cluster ions ($n < 7$) probed with photon energies up to 3.49 eV are observed to decay exclusively by evaporation of either a single neutral atom or a neutral dimer depending on whether they are even or odd size. Large gold cluster ions ($n > 15$) are found to decay by evaporation of neutral monomers, only. In the intermediate size range ($7 \leq n \leq 15$) the even-numbered clusters decay by monomer evaporation, while for the odd-numbered clusters there is an observable competition between monomer and dimer evaporation [13].

So far the studies of decay pathway branching ratios of atomic or molecular clusters, to our knowledge, have not included the excitation energy dependence of the phenomenon. For time-resolved measurements of the energy-dependent decay pathway branching it is essential to perform a well-defined excitation both with respect to time and energy. Therefore, instead of collision-induced dissociation (CID) as applied in [4, 5, 7–12] a 10-ns laser pulse is used for the present investigations. The laser pulse precisely defines both the time of excitation and thus the beginning of the delayed dissociation process and the amount of excitation energy by choice of the respective wavelength. Furthermore, to monitor the statistical unimolecular dissociation process time-resolved, a Penning trap is used for storage before, during and after photoexcitation. It is thus possible to detect the decay products after a well-defined variable time and the procedure allows us to work on timescales which are many orders of magnitude longer than the timescales of cluster equilibration after

✉ Fax: +49-3834/86-4701,
E-mail: lutz.Schweikhard@physik.uni-greifswald.de

excitation. Thus the initial optical excitation is converted into vibrational modes which result in dissociation of the excited clusters.

In the following, we present a quantitative study of the energy dependence of the dimer-to-monomer ratio as a function of excitation energy for those small odd-sized gold clusters Au_n^+ for which a competition between monomer and dimer evaporation is observed. The experimental procedure and results are described in Sects. 2 and 3. The results are found to be in disagreement with the expectations. Thus, in Sect. 4 the relevant theoretical aspects are reviewed and possible explanations of the discrepancies are discussed.

2 Experimental procedure

The experimental setup and various aspects of the use of Penning traps in the field of cluster research have already been described in detail elsewhere [14–17]. For the present experiments, the following procedure has been applied:

- Singly charged cluster ions are produced in a Smalley-type laser vaporization source [18, 19].
- They are transferred to the Penning trap where the cluster ions are captured in flight.
- Selection of the cluster size of interest is achieved by resonant ejection of all other clusters.
- Photoexcitation is then performed by a Nd:YAG pumped 10-ns dye laser pulse at photon energies of 2–6 eV.
- This is followed by a variable, interactionless storage period of up to 60 ms, after which the resulting cluster ion ensemble is ejected from the trap into a time-of-flight (TOF) mass spectrometer equipped with a conversion electrode detector.

This cycle is repeated several hundred times to increase the statistics. By variation of the storage period between photoexcitation and ejection, the delayed dissociation process is monitored time-resolved. As an example, Fig. 1 shows the signal intensity of Au_{13}^+, Au_{12}^+ and Au_{11}^+ as a function of the delay period between photoexcitation and ion detection for the delayed fragmentation of Au_{13}^+ where both the evaporation of monomers and dimers is observed. Note that the decay constants of monomer and dimer evaporation agree within the uncertainties and both types of fragment clusters Au_{12}^+ and Au_{11}^+ are being built up with the same rate constant as the one Au_{13}^+ clusters decay with. A sequential decay where the decay constants agree only accidentally can be excluded since the abundance of Au_{12}^+ at short delay times is not sufficient to explain the increase of the Au_{11}^+ signal. As already discussed in detail for the similar case of Ag_{13}^+ [6], a hypothetical delayed sequential decay would require a corresponding fast dissociation to the intermediate product, which would show up as an offset in the Au_{12}^+ intensity at short delay times.

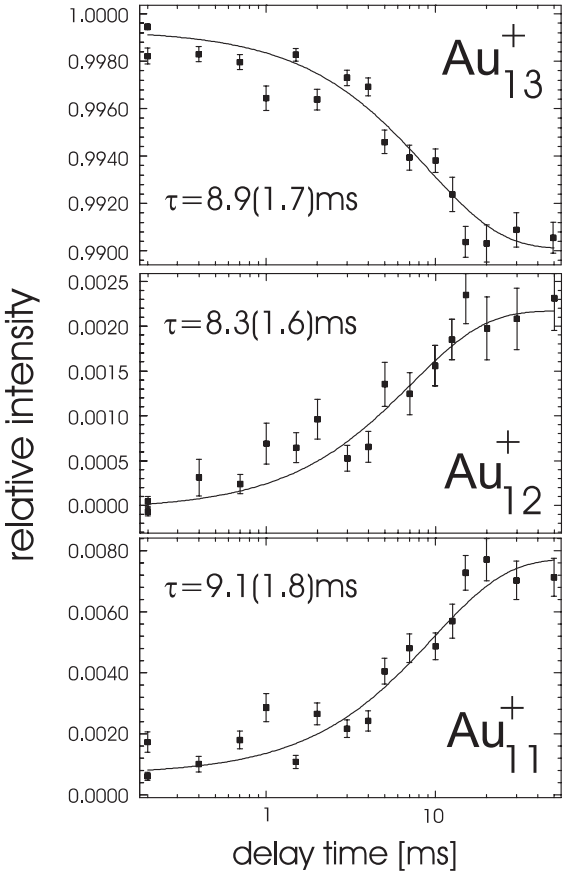

FIGURE 1 Relative cluster intensities as a function of the delay period between photoexcitation and detection. Example of the decay $Au_{13}^+ \rightarrow Au_{12}^+$, Au_{11}^+ after excitation with a 10-ns laser pulse at 4.40 eV photon energy and a pulse energy of 100 μJ

3 Experimental results

Figure 2 shows the relative dimer yield as a function of the storage time in the trap after photoexcitation. As expected, the yield is constant within the statistical uncertainty. In the present case, the relative dimer yield d has the value 0.804(7) and correspondingly the relative monomer yield m is $1-d=0.196(7)$, leading to a dimer-to-monomer-ratio of 4.10(18). For cluster sizes $7 \leq n \leq 15$ delayed photodissociation has been monitored in a time-resolved manner as a function of excitation energy, and the dimer-to-monomer-ratio $d(n, E)/m(E, n)$ has been determined as described above.

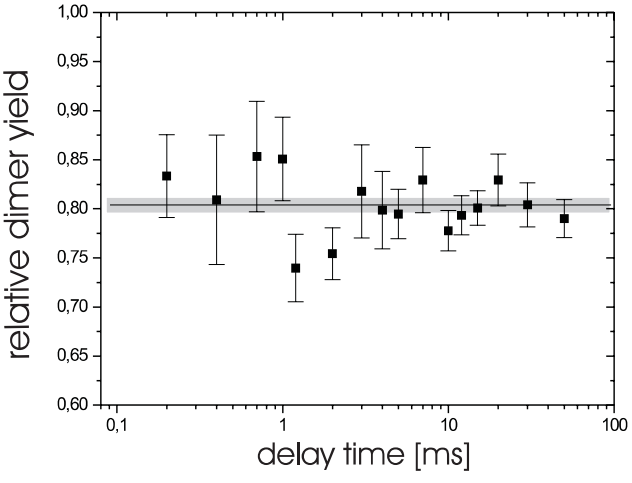

FIGURE 2 Relative dimer yield (data from Fig. 1) as a function of the delay time

When it has been verified that the ratio does not depend on the measurement delay time, as shown in Fig. 2, this ratio of abundancies is identical to the ratio of the corresponding evaporation rates $k_2(E, n)/k_1(E, n)$.

Figure 3 shows the dependence of the dimer-to-monomer ratio on the excitation energy for all cluster sizes where a competition has been observed. In general, the measured ratio decreases with increasing cluster size n. The anomalous behaviour of Au_9^+ in the transition from Au_7^+ to Au_{15}^+ has been rationalized as an effect of the electronic shell closing at $n_e = 8$ atomic valence electrons and can be understood in terms of the liquid drop model with empirical corrections for the odd–even staggering and the shell energy [13].

In addition to the cluster-size dependence, the dimer-to-monomer ratio is in all cases observed to decrease monotonously with increasing excitation energy. This behaviour can be described by the empirical relation

$$\frac{k_2(E,n)}{k_1(E,n)} = \exp\left[s\,(n)\cdot E + s_0(n)\right], \qquad (2)$$

where E is the total excitation energy of the cluster and $s(n)$ and $s_0(n)$ are fit parameters. The values are given in Table 1. Two features in these data deserve particular attention. First, the energy dependence is fairly weak, and second, all the curves have a negative slope, i.e. the relative dimer yield decreases with increasing excitation energy.

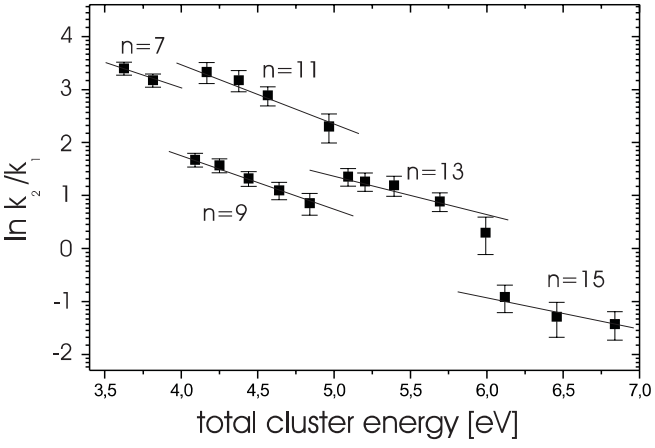

FIGURE 3 Logarithm of the observed dimer-to-monomer ratios as a function of excitation energy for odd-sized clusters Au_n^+, $n = 7$–15. The *lines* through the data points are fits according to (2) with the fit parameters given in Table 1. A thermal room-temperature energy of $(n-2)$ 0.063 eV has been added to the photon energy

n	s [1/eV]	s_0
7	0.93 ± 0.09	6.67 ± 0.31
9	0.98 ± 0.08	5.53 ± 0.27
11	1.13 ± 0.13	7.94 ± 0.44
13	0.75 ± 0.12	5.03 ± 0.42
15	0.59 ± 0.15	2.61 ± 0.34

TABLE 1 Measured slopes $s(n)$ of the energy dependency of $\ln\, k_2/k_1$ for the gold clusters Au_n^+ ($n = 7, 9, 11, 13, 15$). The value s_0 is the corresponding integration constant used in (2)

4 Discussion

4.1 *Review of theoretical aspects*

In order to build the framework for the discussion of these results we will briefly review the expectations and the relevant information available in literature. Given the long timescale in the experiment (compared with electronic and vibrational timescales) the fragmentation process is best described by a statistical theory. The one most directly applicable for handling dimer evaporation seems to be the Weisskopf formula [20] which was originally derived for nuclei but has been applied to clusters on a number of different occasions [21–25]. It is based on detailed balance considerations and describes the rates, and hence yields, as a function of excitation energy E, cluster size n and the dissociation energies D_1 for monomer and D_2 for dimer evaporation [25]

$$k_1(E, D_1, n) = \frac{8\,\pi\, g_1\, \mu_1}{h^3}\, \sigma_{n-1,1}\, T_{n-1}^2\, \frac{\varrho_{n-1}(E - D_1)}{\varrho_n(E)}\,, \qquad (3)$$

$$k_2(E, D_2, n) = \frac{8\,\pi\, g_2\, \mu_2}{h^3}\, \sigma_{n-2,2}\, T_{n-2}^2\, Z\, \frac{\varrho_{n-2}(E - D_2)}{\varrho_n(E)}\,, \qquad (4)$$

where g_j is the electronic degeneracy of the monomer, respectively, dimer, μ_j is the reduced mass of the respective fragment channel, $\sigma_{n-j,j}$ is the capture cross-section for the fragment Au_j^+ by the $(n\text{-}j)$-atomic rest cluster, T_{n-j} (defined below) is the microcanonical temperature of the remaining cluster after evaporation, and ϱ is the level density. The cross-sections can be assumed to be geometric and are thus given by

$$\sigma_{n-j,j} = r_1^2 \pi ((n-j)^{1/3} + j^{1/3})^2, \qquad j = 1, 2\,, \qquad (5)$$

where $r_1 = 1.59$Å is the atomic radius [29]. In the case of dimer evaporation, Z is the rovibrational partition function of the evaporated dimer, which in the rigid-rotator approximation [26] can be factorized into independent rotational and vibrational partition functions of the evaporated dimer [26]. Typically, Z is of the order of 10^4 with the main contribution from the rotational partition function. According to (3) and (4), the frequency factor for dimer evaporation ($\frac{8\,\pi\, g_2\, \mu_2}{h^3}\, \sigma_{n,2}\, T_{n-2}^2\, Z$) is about Z times higher than the frequency factor for monomer evaporation. However, this large enhancement is partly compensated by the larger entropy loss in the dimer evaporation compared to the monomer evaporation.

The analysis of the data is simplified by considering the energy dependence of the branching ratio in the form of the logarithmic derivative with respect to excitation energy. By use of the rate equations (3) and (4), the expression

$$\frac{\mathrm{d}}{\mathrm{d}E}\, \ln \frac{k_2}{k_1} \approx \frac{\mathrm{d}}{\mathrm{d}E}\, \ln\, \frac{\varrho_{n-2}(E - D_2)}{\varrho_{n-1}(E - D_1)} = T_{n-2}^{-1}(E - D_2) - T_{n-1}^{-1}(E - D_1) \qquad (6)$$

can be derived. For the last equality the microcanonical temperature of the cluster after evaporation has been used, as defined by [25]

$$T_{n-j}^{-1} = \frac{\mathrm{d}}{\mathrm{d}E}\, \ln\left(\varrho_{n-j}\left(E - D_j\right)\right) \qquad j = 1, 2\,. \qquad (7)$$

With the assumption that the heat capacity C_n of the cluster scales with the number of vibrational degrees of freedom, one finds

$$\frac{1}{n-4}\int_0^{T_0} C_{n-2}\,\mathrm{d}T = \frac{1}{n-3}\int_0^{T_0} C_{n-1}\,\mathrm{d}T\,. \tag{8}$$

With the further assumption that the heat capacity of the system does not change significantly between the temperatures $T_{n-1}(E-D_1)$ and $T_{n-2}(E-D_2)$, one derives

$$\begin{aligned} E-D_2 &= \int_0^{T_{n-2}} C_{n-2}\,\mathrm{d}T \\ &= (T_{n-2}-T_{n-1})\,C_{n-2} + \frac{n-4}{n-3}\int_0^{T_{n-1}} C_{n-1}\,\mathrm{d}T \\ &= (T_{n-2}-T_{n-1})\,C_{n-2} + \frac{n-4}{n-3}\,(E-D_1), \end{aligned} \tag{9}$$

which can be written as

$$(T_{n-2}-T_{n-1})\,C_{n-2} = \frac{E}{n-3} - (D_2-D_1) - \frac{D_1}{n-3}. \tag{10}$$

This gives the slope of the branching ratio with respect to the energy

$$\begin{aligned} s(n) &:= \frac{\mathrm{d}}{\mathrm{d}E}\,\ln\,\frac{k_2}{k_1} \\ &= \frac{1}{T_{n-1}\,T_{n-2}\,C_{n-2}}\left(D_2-D_1+\frac{D_1-E}{n-3}\right). \end{aligned} \tag{11}$$

This expression takes into account both the difference in dissociation energy for the two channels and the decrease in the number of degrees of freedom during dimer evaporation. Contrary to what the fits to the experimental data in Fig. 3 suggest, the resulting $s(n)$ is not completely independent of the excitation energy. Since the data is not considered to be accurate enough to provide higher-order derivatives we restrict the discussion to the first derivative. (11) can be evaluated by inserting numbers for the heat capacity, which gives the two temperatures and the excitation energy. To be specific the heat capacity can be estimated from bulk values by the scaling

$$C_n = (n-2)\,C_{\mathrm{bulk},N}/N, \tag{12}$$

where 2 is subtracted from n to account for the exterior translational and rotational degrees of freedom of the system.

The resulting difference between dimer and monomer dissociation energies is of the magnitude of the product cluster temperatures, i.e. $D_2-D_1 = O(T_{n-j})$, $(j=1,2)$, for all five cluster sizes under investigation. This can also be seen by use of the following estimate: (11) can be rewritten as

$$s(n)\,T_{n-1}\,T_{n-2}\,C_{n-2} = D_2-D_1+\frac{D_1-E}{n-3}\,. \tag{13}$$

Since $s(n)$ is of order -1 $(\mathrm{eV})^{-1}$ and $T_{n-2}\,C_{n-2}$ is of the order of the excitation energy left after (dimer) evaporation, which is of the order of 1 eV, the left-hand side is of the order of T_{n-1}. The last term on the right-hand side is of the order $-3\,T_{n-1}$ and hence we get that D_2-D_1 is in all cases of the order of a few times T_{n-1}.

4.2 *Comparison between expectations and experimental results*

The small differences in dissociation energies expected from a comparison of (13) and the data do not seem plausible, since it would require a very precise finetuning of the dissociation energies of all the measured cluster sizes. This is unlikely, given that the range covers sizes below, at and above the major shell closing at $n_e = 8$. It is also invalidated by the known dissociation energies for Au_{15}^+ which give a difference of almost 1 eV (see Sect. 4.3) as compared to the Debye crystal value for T_{15-1} of typically 0.09 eV.

Furthermore, also for other sizes, the measured slopes $s(n)$ given in Table 1 are in significant disagreement with values calculated from (11) when the monomer and dimer dissociation energies D_1 and D_2 from an inversion of (3) and (4) are used.

It should be noted that in the above analysis the conclusion that branching ratios and dissociation energies are not related as expected does not depend on the value of the frequency factors since these cancel in the derivation.

There are several potential explanations for the observed discrepancy between the expected and the observed energy dependence of the branching ratio. In calculating the logarithmic slope $s(n)$, two assumptions were made: The heat capacity scales with the number of degrees of freedom of the cluster, and the heat capacity per atom does not change much between the two product cluster temperatures T_{n-1} and T_{n-2}. These two assumptions could be wrong for the same reason, namely that a more or less sharp peak is present in the heat capacity due to the cluster analogue of bulk melting. The potential importance of melting is emphasized by the fact that the parent clusters are excited to or above the melting point if the thermal properties extrapolated from bulk are applied. Furthermore, the melting point of gold clusters is found to be strongly suppressed and size-dependent [30]. Hence even the product clusters may be partly or completely molten. The difference between the monomer and dimer evaporation rates could then be caused by the higher dimer dissociation energy which leads to a lower final temperature of the dimer evaporation product.

However, simulations of the rates with a level density which includes melting, extrapolated from the bulk level density, have so far failed to give a significant improvement in the agreement between the calculated and measured branching ratio. Another argument against melting is the value of the latent heat. Simulations suggest that for clusters containing less than several hundred atoms the latent heat virtually disappears [31]. However, melting effects cannot be positively ruled out since monomer evaporation leads from an electronically even cluster to an odd cluster, while dimer evaporation conserves the even number of electrons.

Finally, the precursor cluster may radiate on the timescale of the experiment. This would cause the measured rate to be some combination of the rate of evaporation and radiative en-

ergy loss. Nevertheless, radiative cooling does not explain the data: radiation essentially quenches the decay and reduces the fragment yield but does not change the ratio of monomer and dimer rate constants which determines the branching ratio.

4.3 *The case of* Au_{15}^+

If we turn to the special case of $n = 15$, where the determination of the dissociation energies D_1 and D_2 does not rely on any expresssion for the rate constant [27], the values of the dissociation energies are 3.52(13) eV and 4.41(17) eV for monomer and dimer evaporation. The latter has been found by application of a Born–Haber cycle for two sequential monomer evaporations and by use of the dimer binding energy of 2.29(2) eV [28]. Here, the only unknown in the expressions (3) and (4) for the rate constants are the level densities. The level density extrapolated from bulk values is close to that of a Debye crystal below the melting point of 1336 K [29] and we can use these values as a reference. This does not account for the electronic degeneracies, or more precisely for the electronic free energy which modifies the dissociation energies. However, it is not expected to be an important correction for $n = 15$, at least not for the discussion of branching ratios, since both the products $n = 14$ and $n = 13$ are mid-shell clusters and also fairly cold compared with the splitting of electronic levels. Since the precursor cluster is hotter, some correction could be relevant for the calculation of absolute rates.

The deviations from harmonic oscillator level densities, including the effect of electronic degeneracies and melting, can be collected into a single empirical correction factor on the rate constant. In bulk equilibrium the factor is $1/80$ on the monomer rate when the harmonic oscillator approximation is used [25]. Comparing the measured rates to the ones calculated with (3) by use of the dissociation energy 3.52 eV gives a correction factor of $1/30$, which is of the same order of magnitude as the bulk value of $1/80$ given above. It is not constant over the whole range of excitation energies (it increases with energy) and varies by a factor 5 within the $1\,\sigma$ error bar of the dissociation energies, but overall it is consistent with the one derived from bulk vapor pressures.

Accordingly, for dimer loss a correction factor of $(1/30)^2$ is expected since twice the atomic entropy is lost in the evaporation. However, the correction factor for dimer evaporation has a value of more than 10 and a strong energy dependence. Hence, the measured dimer evaporation rates are a factor of $10 \times 30^2 \approx 10^4$ higher than the expected values from (4). This discrepancy is obviously reflected in the calculated dimer-to-monomer branching ratios which are less than 10^{-4} and not close to 1 as measured.

Hence for the case of $n = 15$ the monomer rate constant seems well described by the Weisskopf formula but the dimer rate constant fails. This is not the case in general: For other cluster sizes also the monomer rate constant shows serious deviations from both standard and nonstandard formulas linking energies and rates [27].

5 Conclusion

For the first time, the energy dependence of the decay pathway branching ratio between neutral monomer and neutral dimer evaporation from size-selected photoexcited metal clusters has been measured. For gold cluster ions Au_n^+ ($n = 7$, 9, 11, 13 and 15) the corresponding rates of monomer and dimer evaporation have been determined by time-resolved observation of the delayed dissociation. The dimer-to-monomer branching ratio vs. excitation energy is in all cases found to have a negative slope. It is not possible to understand this behaviour in terms of simple unimolecular dissociation theory. This situation is quite similar to previously found results [27] where monomer rates and dissociation energies were compared. It is interesting to note that dissociation energies derived from Arrhenius plots were in general in better agreement with the true values for the odd cluster sizes than for the even ones, suggesting some odd–even variation of the as yet unidentified effect which causes the rate constants to deviate from the predicted values. We expect that a complete understanding of the present data, as well as previous results, requires a more detailed knowledge of the level densities of the involved species than presently available. In summary, several possible explanations of the unexpected fragmentation behaviour have been examined but none of them has been able to explain the data in a consistent and convincing way.

ACKNOWLEDGEMENTS This work is part of the doctoral thesis of M. Vogel and was funded by the DFG and the EU networks "Eurotraps" and "Cluster Cooling". We further thank the Materials Science Research Center at Mainz, the Fonds der Chemischen Industrie and the Academy of Finland under the Finnish Center of Excellence Programme 2000–2005 for financial support.

REFERENCES

1 C. Bréchignac, H. Buscnh, Ph. Cahuzac, J. Leygnier: J. Chem. Phys. **101**, 6992 (1994)
2 C. Bréchignac, Ph. Cahuzac, J. Leygnier, J. Weiner: J. Chem. Phys. **90**, 1492 (1989)
3 C. Bréchignac, Ph. Cahuzac, F. Carlier, M. deFrutos, J. Leygnier: J. Chem. Phys. **93**, 7449 (1990)
4 S. Krückeberg, G. Dietrich, K. Lützenkirchen, L. Schweikhard, C. Walther, J. Ziegler: Int. J. Mass. Spectrom. Ion Proc. **155**, 141 (1996)
5 O. Ingolfsson, U. Busolt, K. Sugawara: J. Chem. Phys. **112**, 4613 (2000)
6 U. Hild, G. Dietrich, S. Krückeberg, M. Lindinger, K. Lützenkirchen, L. Schweikhard, C. Walther, J. Ziegler: Phys. Rev. A **57**, 2786 (1998)
7 S. Becker, G. Dietrich, H.-U. Hasse, N. Klisch, H.-J. Kluge, D. Kreisle, S. Krückeberg, M. Lindinger, L. Schweikhard, H. Weidele, J. Ziegler: Z. Phys. D **30**, 341 (1994)
8 H. Weidele, M. Vogel, A. Herlert, S. Krückeberg, P. Lievens, R.E. Silverans, C. Walther, L. Schweikhard: Eur. Phys. J. D **9**, 173 (1999)
9 V. A Spasov, T.H. Lee, J.P. Maberry, K.M. Ervin: J. Chem. Phys. **110**, 5208 (1999)
10 V.A. Spasov, T.H. Lee, K.M. Ervin: J. Chem. Phys. **112**, 1713 (2000)
11 V.A. Spasov, Y. Shi, K.M. Ervin: Chem. Phys. **262**, 75 (2000)
12 S. Krückeberg, G. Dietrich, K. Lützenkirchen, C. Walther, L. Schweikhard: J. Chem. Phys. **114**, 2955 (2001)
13 M. Vogel, K. Hansen, A. Herlert, L. Schweikhard: Eur. Phys. J. D, in press
14 S. Becker, K. Dasgupta, G. Dietrich, H.-J. Kluge, S. Kusnezov, M. Lindinger, K. Lützenkirchen, L. Schweikhard, J. Ziegler: Rev. Sci. Instrum. **66**, 4902 (1995)
15 L. Schweikhard, S. Becker, K. Dasgupta, G. Dietrich, H.-J. Kluge, D. Kreisle, S. Krückeberg, S. Kusnezov, M. Lindinger, K. Lützenkirchen, B. Obst, C. Walther, H. Weidele: Physica Scripta **T59**, 236 (1995)
16 L. Schweikhard, S. Krückeberg, K. Lützenkirchen, C. Walther: Eur. Phys. J. D **9**, 15 (1999)
17 L. Schweikhard, A. Herlert, M. Vogel: In *The Physics and Chemistry of Clusters* (Proc. Nobel Symp. 117) E.E.B. Campbell, M. Larsson (World Scientific, Singapore 2001) pp. 267–277

18 T. Dietz, M.A. Duncan, D.E. Powers, R.E. Smalley: J. Chem. Phys. **74**, 6511 (1981)
19 H. Weidele, U. Frenzel, T. Leisner, D. Kreisle: Z. Phys. D **20**, 411 (1991)
20 V. Weisskopf, Phys. Rev. **52** , 259 (1937)
21 G.F. Bertsch, N. Oberhofer, S. Stringari: Z. Phys. D **20**, 123 (1991)
22 S. Frauendorf: Z. Phys. D **35**, 191 (1995)
23 P. Fröbich: Phys. Lett. A **202**, 99 (1995)
24 D.H. E Gross: Z. Phys. D **35**, 27 (1995)
25 K. Hansen: Philos. Mag. B **79**, 1413 (1999)
26 D.A. McQuarrie: *Statistical Mechanics* (New York 1976)
27 M. Vogel, K. Hansen, A. Herlert, L. Schweikhard: Phys. Rev. Lett. **87**, 013401 (2001)
28 M.D. Morse: Chem. Rev. **86**, 1049 (1986)
29 C. Kittel: *Introduction to Solid State Physics* (New York 1996)
30 Ph. Buffat, J.-P. Borel: Phys. Rev. A **13**, 6 (1976)
31 F. Ercolessi, W. Andreoni, E. Tosatti: Phys. Rev. Lett. **66**, 911 (1991)